



Detecting a Higgs Pseudoscalar with a Z Boson Produced in Bottom Quark Fusion

Chung Kao* and Shankar Sachithanandam†

*Department of Physics and Astronomy,
University of Oklahoma, Norman, OK 73019, USA*

Abstract

We investigate the prospects of detecting a Higgs pseudoscalar (A^0) in association with a Z gauge boson produced from bottom quark fusion ($b\bar{b} \rightarrow ZA^0$) at the CERN Large Hadron Collider (LHC). A general two Higgs doublet model and the minimal supersymmetric standard model are adopted to study the discovery potential of $pp \rightarrow ZA^0 \rightarrow \ell\bar{\ell}b\bar{b} + X$, $\ell = e$ or μ , via $b\bar{b} \rightarrow ZA^0$ with physics backgrounds and realistic cuts. Promising results are found for $m_A \lesssim 400$ GeV in a general two Higgs doublet model when the heavier Higgs scalar (H^0) can decay into a Z boson and a Higgs pseudoscalar ($H^0 \rightarrow ZA^0$). We compare the production rates from bottom quark fusion ($b\bar{b} \rightarrow ZA^0$) and gluon fusion ($gg \rightarrow ZA^0$), and find that they are complementary processes to produce ZA^0 in hadron collisions. While gluon fusion is the major source for producing a Higgs pseudoscalar associated with a Z boson at the LHC for $\tan\beta \lesssim 10$, bottom quark fusion can make dominant contributions for $\tan\beta \gtrsim 10$.

* E-mail address: Kao@physics.ou.edu

† E-mail address: Shankar@physics.ou.edu

I. INTRODUCTION

In the Standard Model (SM), the Higgs mechanism requires only one Higgs doublet to generate masses for fermions and gauge bosons. It leads to the appearance of a neutral CP-even Higgs scalar after spontaneous electroweak symmetry breaking. The LEP2 experiments have established a lower bound of 114.4 GeV [1] for the SM Higgs boson mass at 95% confidence level.

A two Higgs doublet model (2HDM) [2] has Higgs doublets ϕ_1 and ϕ_2 with the vacuum expectation values v_1 and v_2 . There are five physical Higgs bosons: a pair of singly charged Higgs bosons H^\pm , two neutral CP-even scalars H^0 (heavier) and h^0 (lighter), and a neutral CP-odd pseudoscalar A^0 . The couplings of the Higgs bosons to fermions and gauge bosons depend on the ratio of vacuum expectation values ($\tan\beta \equiv v_2/v_1$) and a mixing angle (α_H) between the weak and mass eigenstates of the neutral scalars.

The supersymmetry between a boson and a fermion preserves the elementary nature of Higgs bosons. The minimal supersymmetric standard model (MSSM) [3] requires two Higgs doublets ϕ_1 and ϕ_2 coupling to fermions with weak isospin $t_3 = -1/2$ and $t_3 = +1/2$ respectively, to generate masses for fermions and gauge bosons and to cancel triangle anomalies associated with the fermionic partners of the Higgs bosons. The Higgs potential is constrained by supersymmetry such that all tree-level Higgs boson masses and couplings are determined by just two independent parameters, commonly chosen to be the mass of the CP-odd pseudoscalar (m_A) and $\tan\beta$. The mixing angle α_H between the neutral scalars is often chosen to be negative ($-\pi/2 \leq \alpha_H \leq 0$). The LEP2 collaborations have set a lower bound of 91 GeV and 91.9 GeV [4] for the m_h and the m_A , respectively.

Extensive studies have been made for the detection of a heavier MSSM Higgs boson ($\phi^0 = H^0$ or A^0) at the CERN LHC [5, 6, 7, 8, 9, 10, 11, 12, 13, 14, 15, 16]. For $\tan\beta \lesssim 5$, $A^0 \rightarrow \gamma\gamma$, $H^0 \rightarrow ZZ^* \rightarrow 4\ell$, and $A^0, H^0 \rightarrow t\bar{t}$ are possible discovery channels. In the SM, $H \rightarrow ZZ^* \rightarrow 4\ell$ offers great promise for $160 \text{ GeV} \lesssim m_H \lesssim 1 \text{ TeV}$ [14, 15, 16] with physics background from $q\bar{q} \rightarrow ZZ$ [17] and $gg \rightarrow ZZ$ [18, 19]. However, the heavy scalar in the MSSM is observable via $H^0 \rightarrow ZZ^*$ only for $\tan\beta \lesssim 10$ and $m_A \lesssim 350 \text{ GeV}$ [7]. The detection modes $A^0 \rightarrow Zh^0 \rightarrow l^+l^-\tau\bar{\tau}$ [10] or $l^+l^-b\bar{b}$ [10, 14, 16] and $H^0 \rightarrow h^0h^0 \rightarrow bb\gamma\gamma$ [16] may be promising channels for simultaneous discovery of two Higgs bosons in the MSSM. For large values of $\tan\beta$, $\phi^0 \rightarrow \mu\bar{\mu}$ [11, 12, 13, 14, 16], and $\phi^0 \rightarrow \tau\bar{\tau}$ [8, 14, 15, 16], are promising discovery channels for the A^0 and the H^0 . In some regions of parameter space, the rates for Higgs boson decays to neutralinos ($H^0, A^0 \rightarrow \chi_2^0\chi_2^0$) are dominant and they might open up new promising modes for Higgs detection [9].

In two Higgs doublet models, there are two complementary channels to search for a Higgs scalar and a Higgs pseudoscalar simultaneously: (i) $A^0 \rightarrow Zh^0$ [10, 14, 16] with a coupling proportional to $\cos(\beta - \alpha_H)$ and (ii) $H^0 \rightarrow ZA^0$ with a coupling proportional to $\sin(\beta - \alpha_H)$. At the LHC, gluon fusion can be a significant source to produce a Higgs pseudoscalar (A^0) and a Z boson ($gg \rightarrow ZA^0$) via triangle and box diagrams with the third generation quarks [20, 21]. The top quark loop diagrams make dominant contribution to $gg \rightarrow ZA^0$ for $\tan\beta \lesssim 10$ [20].

In the MSSM and a 2HDM with Model II Yukawa interactions [22] for the Higgs bosons and fermions, one Higgs doublet (ϕ_1) couples to down-type quarks and charged leptons while another doublet (ϕ_2) couples to up-type quarks and neutrinos. The $A^0b\bar{b}$ coupling is proportional to $\tan\beta$ and this coupling can be greatly enhanced by a large value of $\tan\beta$. In addition, the Higgs pseudoscalar does not couple to gauge boson pairs at the tree level.

Therefore, $A^0 \rightarrow b\bar{b}$ is the dominant decay channel for $\tan\beta \gtrsim 10$ or for $m_A \lesssim m_Z + m_h \sim 210$ GeV with $\tan\beta \sim 2$. Recently, we demonstrated that gluon fusion could be a promising production mechanism to detect $pp \rightarrow ZA^0 \rightarrow \ell\bar{\ell}b\bar{b} + X$ via $gg \rightarrow ZA^0$ for $\tan\beta \sim 2$ and $m_A \lesssim 260$ GeV [23].

In this article, the prospects of the search for a Higgs pseudoscalar (A^0) associated with a Z boson produced are investigated. We study the discovery potential of $pp \rightarrow ZA^0 \rightarrow \ell\bar{\ell}b\bar{b} + X$ via bottom quark fusion ($b\bar{b} \rightarrow ZA^0$) at the LHC. The production cross sections of ZA^0 at the LHC in a two Higgs doublet model and the MSSM are discussed in Section II. The dominant physics backgrounds from production of $\ell\bar{\ell}b\bar{b}$ and $W^+W^-b\bar{b}$ are presented in Section III. The discovery potential of $ZA^0 \rightarrow \ell\bar{\ell}b\bar{b}$ is discussed in Section IV. Conclusions are drawn in Section V.

II. THE PRODUCTION CROSS SECTIONS

We calculate the cross section for $pp \rightarrow ZA^0 + X$ via $b\bar{b} \rightarrow ZA^0$ in a two Higgs doublet model and the minimal supersymmetric standard model with Model II Yukawa interactions for the Higgs bosons and fermions. The parton distribution functions of CTEQ6L1 [24] are employed to evaluate the cross section for $pp \rightarrow ZA^0 \rightarrow \ell\bar{\ell}b\bar{b} + X$ with the Higgs production cross section $\sigma(pp \rightarrow ZA^0 + X)$ multiplied by the branching fractions of $Z \rightarrow \ell\bar{\ell}$ and $A^0 \rightarrow b\bar{b}$. In the Yukawa couplings of $\phi^0 b\bar{b}$ ($\phi^0 = A^0, H^0, h^0$), the bottom quark mass is chosen to be the next-to-leading order (NLO) running mass $m_b(m_A)$ [25], which is calculated with $m_b(\text{pole}) = 4.7$ GeV and the NLO evolution of the strong coupling [26].

In Figure 1, we present the Feynman diagrams for $b\bar{b} \rightarrow ZA^0$. The s-channel diagrams contain the heavy Higgs scalar H^0 [$g_{AZH} \propto \sin(\beta - \alpha_H)$] and the light Higgs scalar h^0 [$g_{AZh} \propto \cos(\beta - \alpha_H)$] in the intermediate state. Therefore, this discovery channel might provide a good opportunity to measure the couplings of ZH^0A^0 and Zh^0A^0 . The t and u channel diagrams are proportional to $\tan\beta$. When the t and u channel diagrams dominate, the cross section of $b\bar{b} \rightarrow ZA^0$ can be enhanced by a large value of $\tan^2\beta$. We have checked the relevant couplings with the unitarity condition for the total amplitude. At very high energy, the longitudinal polarization vector (ϵ_μ) of the Z boson can be expressed as the momentum vector over Z mass (p_μ/M_Z). Then unitarity requires cancellation among the s , t , and u channel diagrams at high energy.

Figure 2 presents the cross section of $pp \rightarrow ZA^0 \rightarrow \ell\bar{\ell}b\bar{b} + X$ via $b\bar{b} \rightarrow ZA^0$ as a function of $\tan\beta$ in a general two Higgs doublet model and the minimal supersymmetric standard model. We have chosen $m_H = m_A + 100$ GeV, $m_h = 120$ GeV, and $\alpha_H = -\pi/4$ for the general 2HDM. It is clear that the cross section in a 2HDM can be significantly larger than that in the the MSSM when the H^0 can decay into ZA^0 with $m_H > m_A + M_Z$ since m_H and α_H are free parameters in a 2HDM. In the MSSM with $\tan\beta \gtrsim 10$, m_A and m_h are very close to each other for $m_A \lesssim 125$ GeV, while m_A and m_H are almost degenerate when $m_A \gtrsim 125$ GeV [11]. Therefore, the decay $H^0 \rightarrow ZA^0$ is kinematically inaccessible in the MSSM. The cross section for gluon fusion alone is also presented in this figure. While gluon fusion is the major source for producing ZA^0 with $\tan\beta \lesssim 10$, bottom quark fusion can make dominant contribution for $\tan\beta \gtrsim 10$.

The Higgs production rate via bottom quark fusion is very sensitive to the choice of factorization scale (μ_F) [27, 28, 29]. In Table I we present the cross section of $pp \rightarrow ZA^0 \rightarrow \ell\bar{\ell}b\bar{b} + X$ via $b\bar{b} \rightarrow ZA^0$ in a two Higgs doublet model with $\tan\beta = 10$ and several values of m_A for $\mu_F = M_Z + m_A, (M_Z + m_A)/2, (M_Z + m_A)/4$. In our analysis, we have chosen

$\mu_F = M_Z + m_A$ with the running bottom quark mass $m_b(m_A)$ in the Yukawa couplings. Our numerical values of cross section are comparable to the recent next-to-leading order QCD predictions for $Z^0 A^0$ associated production [30].

TABLE I: The cross section in fb without cuts for $pp \rightarrow ZA^0 + X \rightarrow \ell\bar{\ell}b\bar{b} + X$ via bottom quark fusion ($b\bar{b} \rightarrow ZA^0$) at $\sqrt{s} = 14$ TeV. We choose three values of the factorization scale (μ_F) for $\tan\beta = 10$ and several values of m_A in a two Higgs doublet model with $m_h = 120$ GeV, $m_H = m_A + 100$ GeV and $\alpha_H = -\pi/4$.

$\mu_F \backslash m_A$ (GeV)	100	200	300	400	500
$M_Z + m_A$	28.3	1.81	8.72×10^{-2}	9.19×10^{-3}	1.92×10^{-3}
$(M_Z + m_A)/2$	22.3	1.52	7.58×10^{-2}	8.19×10^{-3}	1.74×10^{-3}
$(M_Z + m_A)/4$	16.1	1.19	6.25×10^{-2}	6.99×10^{-3}	1.53×10^{-3}

To study the effects of the Higgs scalar mixing angle (α_H) in a two Higgs doublet model, we show the cross section of $pp \rightarrow ZA^0 + X \rightarrow \ell\bar{\ell}b\bar{b} + X$ versus α_H in Figure 3 for $\tan\beta = 2, 10, \text{ and } 50$ as well as (a) $m_A = 150$ GeV and (b) $m_A = 400$ GeV. Also shown are the cross sections in the MSSM for $\tan\beta = 2, 10, \text{ and } 50$. In the MSSM, α_H becomes almost zero for $\tan\beta \sim 50$. For $\alpha_H < 0$, the cross section in a 2HDM is significantly larger than that in the MSSM. We include contributions from both bottom quark fusion ($b\bar{b} \rightarrow ZA^0$) and gluon fusion ($gg \rightarrow ZA^0$).

For $m_A > m_Z + m_h$ and $m_A > m_t + m_W$, the branching fraction of $A^0 \rightarrow b\bar{b}$ is suppressed by $A^0 \rightarrow Zh^0$ and $A^0 \rightarrow t\bar{t}^*$ with real and virtual top quarks. Therefore, the cross section of $pp \rightarrow ZA^0 \rightarrow \ell\bar{\ell}b\bar{b} + X$ for $m_A = 400$ GeV is much smaller than that for $m_A = 150$ GeV.

III. THE PHYSICS BACKGROUND

The dominant physics backgrounds to the final state of $ZA^0 \rightarrow \ell\bar{\ell}b\bar{b}$ come from $gg \rightarrow \ell\bar{\ell}b\bar{b}$, $q\bar{q} \rightarrow \ell\bar{\ell}b\bar{b}$, $\ell = e$ or μ and $pp \rightarrow W^+W^-b\bar{b} + X$. In our analysis, we actually evaluated $gg \rightarrow b\bar{b} + \nu\bar{\nu}$ and $q\bar{q} \rightarrow b\bar{b} + \nu\bar{\nu}$ with dominant contribution from $pp \rightarrow t\bar{t} \rightarrow bW^+bW^- + X$. In addition, we also consider backgrounds from $pp \rightarrow \ell\bar{\ell}g\bar{b} + X$, $pp \rightarrow \ell\bar{\ell}g\bar{q} + X$, $pp \rightarrow \ell\bar{\ell}gq + X$, $pp \rightarrow \ell\bar{\ell}g\bar{q} + X$, and $pp \rightarrow \ell\bar{\ell}jj + X$, where $q = u, d, s, \text{ or } c$ and $j = g, q$ or \bar{q} . The programs MADGRAPH [31] and HELAS [32] are employed to evaluate the cross sections for all physics backgrounds.

For an integrated luminosity (L) of 30 fb^{-1} , we require two isolated leptons with $p_T(\ell) > 15$ GeV and $|\eta(\ell)| < 2.5$ in each event. All jets are required to have $p_T(b, j) > 15$ GeV and $|\eta(b, j)| < 2.5$. The b -tagging efficiency (ϵ_b) is taken to be 60%; the probability that a c -jet mistagged as a b -jet (ϵ_c) is 10%, and the probability that any other jet mistagged as a b -jet (ϵ_j) is taken to be 1%. Furthermore, we require the invariant mass of the lepton pairs with opposite signs to be within 10 GeV of M_Z , that is $|M_{\ell\bar{\ell}} - M_Z| \leq 10$ GeV to be the signature of a Z boson.

For a higher integrated luminosity of 300 fb^{-1} , we require the same acceptance cuts as those for $L = 30 \text{ fb}^{-1}$, except $p_T(\ell) > 25$ GeV and $p_T(b, j) > 30$ GeV. The b -tagging efficiency (ϵ_b) is taken to be 50%, and the probability that a c -jet mistagged as a b -jet (ϵ_c) is 14%. We found that the p_T cuts on leptons and bottom quarks are effective in removing most of the SM background, while most leptons from the Z decays and most bottom quarks from the Higgs decays survive the p_T cuts [23].

In addition, we require that the missing transverse energy (\cancel{E}_T) in each event should be less than 20 GeV for $L = 30 \text{ fb}^{-1}$ and less than 40 GeV for $L = 300 \text{ fb}^{-1}$. This cut on missing E_T along with the requirement on the invariant mass of lepton pairs ($|M_{\ell\bar{\ell}} - M_Z| \leq 10 \text{ GeV}$) effectively reduce the background from $pp \rightarrow W^+W^-b\bar{b} + X$ which receives the major contribution from $pp \rightarrow t\bar{t} + X$. Our acceptance cuts and efficiencies of b -tagging and mistagging are similar to those of the ATLAS collaboration [16].

IV. THE DISCOVERY POTENTIAL AT THE LHC

To study the discovery potential of $pp \rightarrow ZA^0 \rightarrow \ell\bar{\ell}b\bar{b} + X$ at the LHC, we calculate the background from the SM processes of $pp \rightarrow \ell\bar{\ell}b\bar{b} + X$ in the mass window of $m_A \pm \Delta M_{b\bar{b}}$ with $\Delta M_{b\bar{b}} = 22 \text{ GeV}$.

We consider the Higgs signal to be observable if the $N\sigma$ lower limit on the signal plus background is larger than the corresponding upper limit on the background [5, 33], namely,

$$L(\sigma_S + \sigma_B) - N\sqrt{L(\sigma_S + \sigma_B)} > L\sigma_B + N\sqrt{L\sigma_B} \quad (1)$$

which corresponds to

$$\sigma_S > \frac{N^2}{L} \left[1 + 2\sqrt{L\sigma_B/N} \right]. \quad (2)$$

Here L is the integrated luminosity, σ_S is the cross section of the Higgs signal, and σ_B is the background cross section within a bin of width $\pm\Delta M_{b\bar{b}}$ centered at m_A . In this convention, $N = 2.5$ corresponds to a 5σ signal.

In CP-conserving two Higgs doublet models with $m_A \gg M_Z$, a CP-even neutral Higgs boson with Standard-Model-like couplings may be the lightest scalar. In this decoupling limit [34], $\sin^2(\beta - \alpha_H) \rightarrow 1$ and $\cos^2(\beta - \alpha_H) \rightarrow 0$. We show the cross section with acceptance cuts in Figure 4 for $pp \rightarrow ZA^0 \rightarrow \ell\bar{\ell}b\bar{b} + X$ in a 2HDM with $m_H = m_A + 100 \text{ GeV}$, $m_h = 120 \text{ GeV}$, and $\alpha_H = \beta - \pi/2$ as well as the cross section in the MSSM, for $L = 30 \text{ fb}^{-1}$ and $L = 300 \text{ fb}^{-1}$. The curves for the 5σ and 3σ cross sections for the ZA^0 signal are also presented. We include contributions from both bottom quark fusion and gluon fusion. With a luminosity of 30 fb^{-1} , it is possible to establish a 5σ signal of $ZA^0 \rightarrow \ell\bar{\ell}b\bar{b}$ for $m_A \lesssim 200 \text{ GeV}$ and $\tan\beta \sim 2$ or $\tan\beta \sim 50$. At a higher luminosity of 300 fb^{-1} the discovery potential of this channel is greatly improved for $m_A \lesssim 280 \text{ GeV}$ and $\tan\beta \sim 2$ or $\tan\beta \sim 50$. In the MSSM, it is difficult to observe the Higgs signal of ZA^0 since $m_H \sim m_A$. In both models, if $m_A > 250 \text{ GeV}$ and $\tan\beta \lesssim 7$, the branching fraction of $A^0 \rightarrow b\bar{b}$ is greatly suppressed when the Higgs pseudoscalar decays dominantly into Zh^0 and $t\bar{t}^*$ with one of the top quarks being virtual.

In Tables II and III, we present event rates after acceptance cuts for the Higgs signal (N_S) from $b\bar{b} \rightarrow ZA^0 \rightarrow \ell\bar{\ell}b\bar{b}$ and the background (N_B) as well as the ratio of signal to background N_S/N_B and $N_S/\sqrt{N_B}$ in a two Higgs doublet model with $\tan\beta = 10$ and 50 , $\alpha_H = -\pi/4$.

The discovery contours for $pp \rightarrow ZA^0 \rightarrow \ell\bar{\ell}b\bar{b} + X$ via $b\bar{b} \rightarrow ZA^0$ at the LHC are presented in Figure 5 for an integrated luminosity of (a) $L = 30 \text{ fb}^{-1}$ and (b) $L = 300 \text{ fb}^{-1}$. We show 5σ contours in the $(\alpha_H, \tan\beta)$ plane for $m_A = 150, 250$ and 400 GeV in a general two Higgs doublet model with $m_h = 120 \text{ GeV}$ and $m_H = m_A + 100 \text{ GeV}$. In addition, we present the curve for the decoupling limit with $\beta - \alpha_H = \pi/2$. For $L = 30 \text{ fb}^{-1}$, it will be possible to

TABLE II: Event rates after acceptance cuts for the Higgs signal ($N_S = \sigma_S \times L$) from $b\bar{b} \rightarrow ZA^0$ and the background ($N_B = \sigma_B \times L$) as well as the ratio of signal to background N_S/N_B and $N_S/\sqrt{N_B}$ in a two Higgs doublet model with $\tan\beta = 10$ and 50 , $\alpha_H = -\pi/4$, and $m_H = m_A + 100$ GeV for an integrated luminosity of 30 fb^{-1} .

$\tan\beta = 10$				
m_A (GeV)	N_S	N_B	N_S/N_B	$N_S/\sqrt{N_B}$
100	196	1.01×10^4	0.019	1.95
200	14	2100	0.007	0.30
300	1	577	0.001	0.03
400	< 1	193	< 0.001	< 0.01
$\tan\beta = 50$				
m_A (GeV)	N_S	N_B	N_S/N_B	$N_S/\sqrt{N_B}$
100	773	1.01×10^4	0.076	7.7
200	138	2100	0.066	3.0
300	31	577	0.054	1.3
400	9	193	0.045	0.62

TABLE III: The same as in Table I, except that the integrated luminosity is 300 fb^{-1} .

$\tan\beta = 10$				
m_A (GeV)	N_S	N_B	N_S/N_B	$N_S/\sqrt{N_B}$
100	897	2.62×10^4	0.034	5.5
200	75	1.02×10^4	0.007	0.74
300	4	3380	0.001	0.06
400	< 1	1170	< 0.001	0.01
$\tan\beta = 50$				
m_A (GeV)	N_S	N_B	N_S/N_B	$N_S/\sqrt{N_B}$
100	3310	2.62×10^4	0.13	20.5
200	731	1.02×10^4	0.07	7.2
300	168	3380	0.05	2.9
400	46	1170	0.04	1.4

discover the ZA^0 signal for $|\alpha_H| \lesssim 0.5$ and $m_A \lesssim 250$ GeV. The higher luminosity ($L = 300 \text{ fb}^{-1}$) greatly improves the reach for m_A up to 400 GeV in a large region of the parameter space with $|\alpha_H| \lesssim 1$.

V. CONCLUSIONS

Bottom quark fusion and gluon fusion are complementary processes to produce a Higgs pseudoscalar (A^0) and a Z boson at the LHC. While gluon fusion is the major source of ZA^0 for $\tan\beta \lesssim 10$, bottom quark fusion can make dominant contributions to the production of ZA^0 at the LHC for $\tan\beta \gtrsim 10$.

We have found promising results for $pp \rightarrow ZA^0 \rightarrow \ell\bar{\ell}b\bar{b} + X$ via $b\bar{b} \rightarrow ZA^0$ in two Higgs

doublet models at the LHC with $L = 300 \text{ fb}^{-1}$ for $m_A \lesssim 400 \text{ GeV}$, $\tan\beta \gtrsim 5$, $|\alpha_H| \lesssim 1$, and $m_H = m_A + 100 \text{ GeV}$. In the MSSM with $m_A \gtrsim 125 \text{ GeV}$, $m_A \sim m_H$, and the production cross section of $gg \rightarrow ZA^0$ is usually small.

Gluon fusion ($gg \rightarrow ZA^0$) offers great promise for $m_A \lesssim 260 \text{ GeV}$ and $\tan\beta \sim 2$ [23]. The production rate of ZA^0 from gluon fusion at the LHC is suppressed by the destructive interference between the triangle and the box diagrams as well as the negative interference between the top quark and the bottom quark loops, especially when they are comparable with $\tan\beta \sim 7$ [20].

In a general two Higgs doublet model, the cross section of $b\bar{b} \rightarrow ZA^0$ and $gg \rightarrow ZA^0$ can be greatly enhanced when the heavier Higgs scalar (H^0) can decay into the Higgs pseudoscalar and a Z boson. If we take $m_H \sim m_A$ in a 2HDM, the Higgs signal will be reduced to the level of the MSSM. This discovery channel might provide a good opportunity to discover two Higgs bosons simultaneously if the heavier Higgs scalar (H^0) can decay into a Z boson and a Higgs pseudoscalar (A^0).

ACKNOWLEDGMENTS

We are grateful to Sally Dawson and Michael Spira for beneficial discussions. This research was supported in part by the U.S. Department of Energy under grants No. DE-FG02-04ER41305 and No. DE-FG02-03ER46040.

REFERENCES

- [1] The LEP Higgs working group, <http://lephiggs.web.cern.ch/LEPHIGGS/www/>; LHWG note 2002-01.
- [2] J. Gunion, H. Haber, G. Kane and S. Dawson, *The Higgs Hunter's Guide* (Addison-Wesley, Redwood City, CA, 1990).
- [3] H.P. Nilles, Phys. Rep. **110** (1984) 1; H. Haber and G. Kane, Phys. Rep. **117** (1985) 75.
- [4] The LEP Higgs working group, <http://lephiggs.web.cern.ch/LEPHIGGS/www/>; LHWG note 2001-04.
- [5] H. Baer, M. Bisset, C. Kao and X. Tata, Phys. Rev. D **46**, 1067 (1992).
- [6] V. D. Barger, M. S. Berger, A. L. Stange and R. J. Phillips, Phys. Rev. D **45**, 4128 (1992); J. F. Gunion and L. H. Orr, Phys. Rev. D **46**, 2052 (1992).
- [7] J. F. Gunion, R. Bork, H. E. Haber and A. Seiden, Phys. Rev. D **46**, 2040 (1992).
- [8] Z. Kunszt and F. Zwirner, Nucl. Phys. B **385**, 3 (1992).
- [9] H. Baer, M. Bisset, D. Dicus, C. Kao and X. Tata, Phys. Rev. D **47**, 1062 (1993); H. Baer, M. Bisset, C. Kao and X. Tata, Phys. Rev. D **50**, 316 (1994).
- [10] H. Baer, C. Kao and X. Tata, Phys. Lett. B **303**, 284 (1993); S. Abdullin, H. Baer, C. Kao, N. Stepanov and X. Tata, Phys. Rev. D **54**, 6728 (1996).
- [11] C. Kao and N. Stepanov, Phys. Rev. D **52**, 5025 (1995).
- [12] S. Dawson, D. Dicus and C. Kao, Phys. Lett. B **545**, 132 (2002).
- [13] S. Dawson, D. Dicus, C. Kao and R. Malhotra, Phys. Rev. Lett. **92**, 241801 (2004).
- [14] CMS Technical Proposal, CERN/LHCC 94-38 (1994).
- [15] Atlas Technical Proposal, CERN/LHCC 94-43 (1994).
- [16] E. Richter-Was, D. Froidevaux, F. Gianotti, L. Poggioli, D. Cavalli and S. Resconi, Int. J. Mod. Phys. A **13**, 1371 (1998); ATLAS Detector and Physics Performance Technical Design Report, CERN/LHCC 99-14/15 (1999).
- [17] R. W. Brown and K. O. Mikaelian, Phys. Rev. D **19**, 922 (1979).
- [18] D. A. Dicus, C. Kao and W. W. Repko, Phys. Rev. D **36**, 1570 (1987).
- [19] E. W. N. Glover and J. J. van der Bij, Nucl. Phys. B **321**, 561 (1989).
- [20] C. Kao, Phys. Rev. D **46**, 4907 (1992).
- [21] J. Yin, W. G. Ma, R. Y. Zhang and H. S. Hou, Phys. Rev. D **66**, 095008 (2002).
- [22] J. F. Donoghue and L. F. Li, Phys. Rev. D **19**, 945 (1979); L. J. Hall and M. B. Wise, Nucl. Phys. B **187**, 397 (1981).
- [23] C. Kao, G. Lovelace and L. H. Orr, Phys. Lett. B **567**, 259 (2003).
- [24] J. Pumplin, D. R. Stump, J. Huston, H. L. Lai, P. Nadolsky and W. K. Tung, JHEP **0207**, 012 (2002).
- [25] J. A. M. Vermaseren, S. A. Larin and T. van Ritbergen, Phys. Lett. B **405**, 327 (1997).
- [26] W. J. Marciano, Phys. Rev. D **29**, 580 (1984).
- [27] F. Maltoni, Z. Sullivan and S. Willenbrock, Phys. Rev. D **67**, 093005 (2003).
- [28] R. V. Harlander and W. B. Kilgore, Phys. Rev. D **68**, 013001 (2003).
- [29] J. Campbell *et al.*, arXiv:hep-ph/0405302.
- [30] Q. Li, C. S. Li, J. J. Liu, L. G. Jin and C. P. Yuan, arXiv:hep-ph/0501070.
- [31] MADGRAPH, by T. Stelzer and W.F. Long, Comput. Phys. Commun. **81**, 357 (1994).

- [32] HELAS, by H. Murayama, I. Watanabe and K. Hagiwara, KEK report KEK-91-11 (1992).
- [33] N. Brown, Z. Phys. **C49** (1991) 657.
- [34] J. F. Gunion and H. E. Haber, Phys. Rev. D **67**, 075019 (2003).

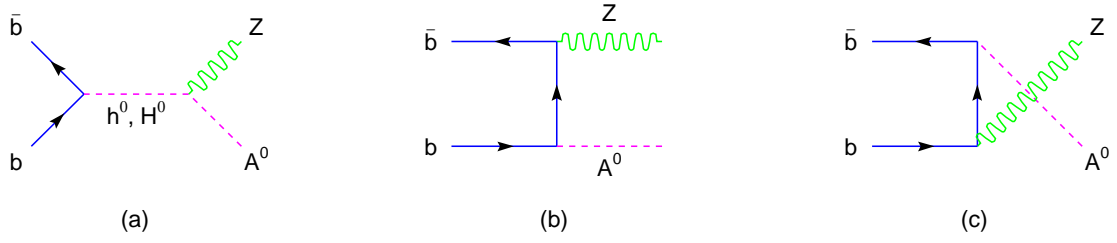


FIG. 1: Feynman diagrams for the signal from $b\bar{b} \rightarrow ZA^0$.

$$\sqrt{s} = 14 \text{ TeV}$$

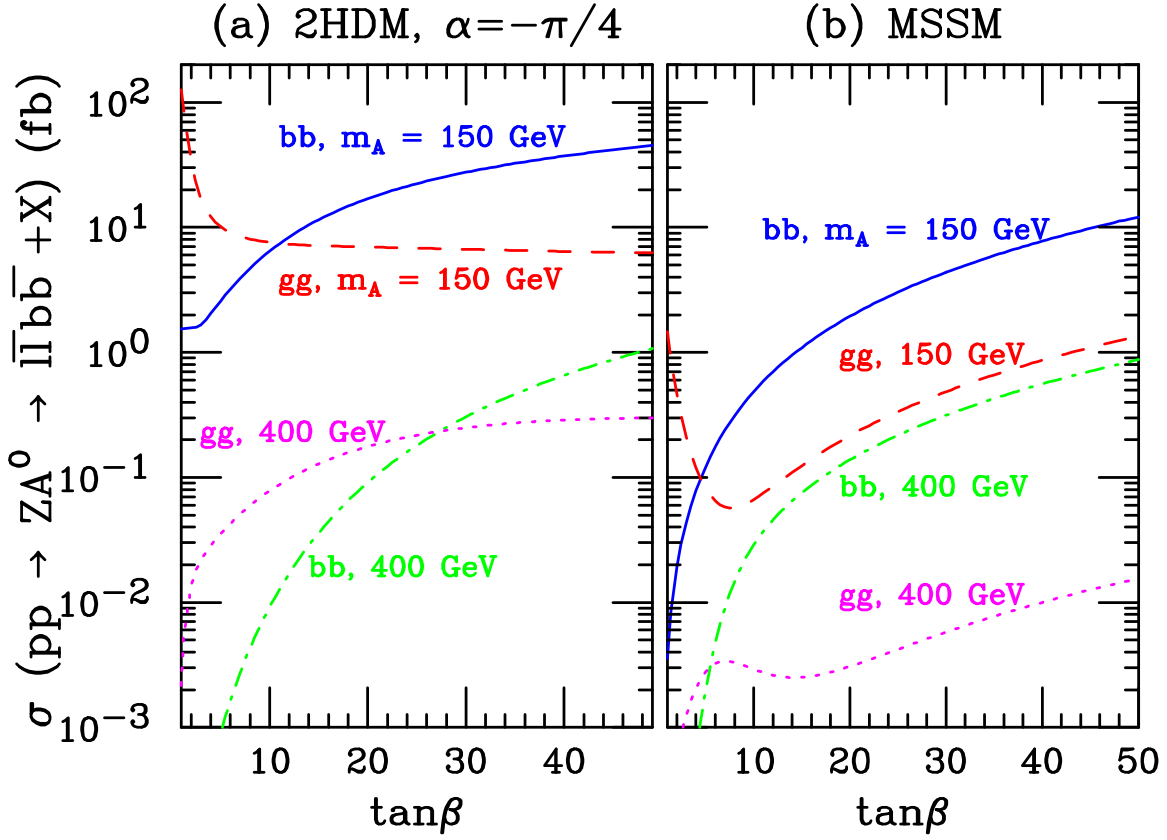


FIG. 2: The cross section in fb without cuts for $pp \rightarrow ZA^0 + X \rightarrow \ell\bar{\ell}b\bar{b} + X$ at $\sqrt{s} = 14$ TeV, as a function of $\tan\beta$, for $m_A = 150$ and 400 GeV, in (a) a two Higgs doublet model with $m_h = 120$ GeV, $m_H = m_A + 100$ GeV and $\alpha_H = -\pi/4$ as well as in (b) the MSSM with $m_{\tilde{q}} = m_{\tilde{g}} = \mu = 1$ TeV. We show contributions from bottom quark fusion ($b\bar{b} \rightarrow ZA^0$) and gluon fusion ($gg \rightarrow ZA^0$) separately.

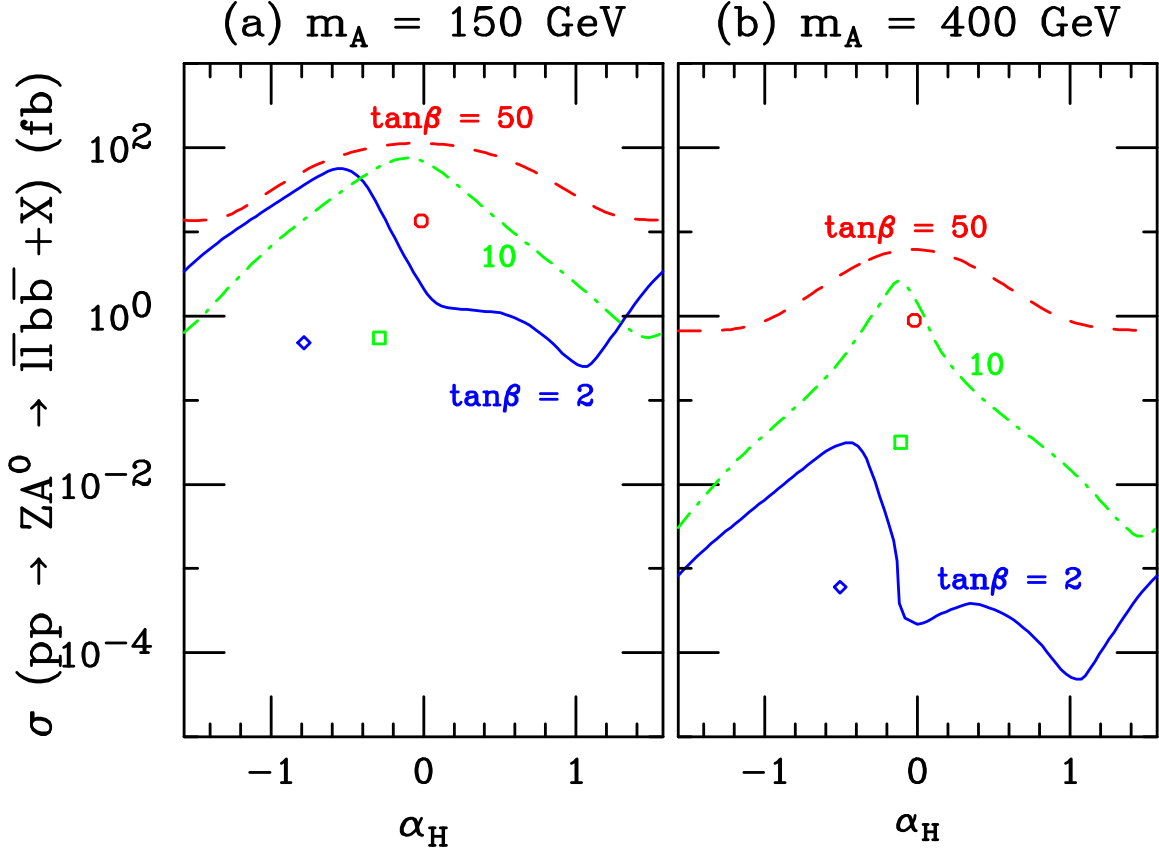


FIG. 3: The cross section in fb without cuts for $pp \rightarrow ZA^0 + X \rightarrow \ell\bar{\ell}b\bar{b} + X$ at $\sqrt{s} = 14$ TeV, as a function of the Higgs scalar mixing angle α_H , in a two Higgs doublet model with $m_h = 120$ GeV, $m_H = m_A + 100$ GeV with $\tan\beta = 2, 10$, and 50 , for (a) $m_A = 150$ GeV and (b) $m_A = 400$ GeV. Also shown are the cross sections in the MSSM for $\tan\beta = 2$ (diamond), 10 (square), and 50 (circle). We include contributions from bottom quark fusion ($b\bar{b} \rightarrow ZA^0$) and gluon fusion ($gg \rightarrow ZA^0$).

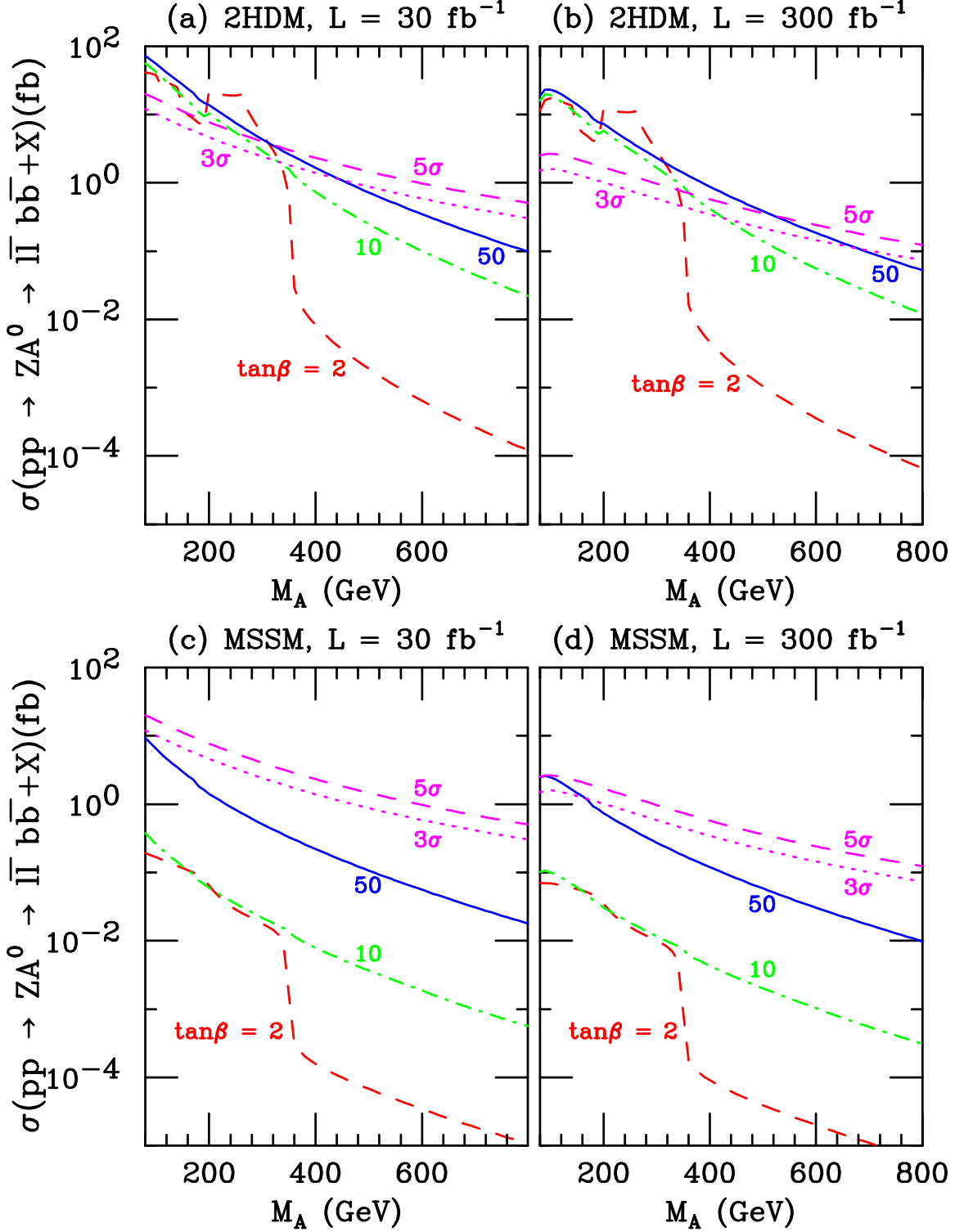


FIG. 4: The cross section in fb for $pp \rightarrow ZA^0 + X \rightarrow \ell\bar{\ell}b\bar{b} + X$ versus m_A at $\sqrt{s} = 14 \text{ TeV}$, in a two Higgs doublet model with $m_h = 120 \text{ GeV}$, $m_H = m_A + 100 \text{ GeV}$ and $\alpha_H = \beta - \pi/2$ (the decoupling limit), for $\tan\beta = 2$ (dashed), 10 (dot-dashed), and 50 (solid). Also shown are the 5 σ (dashed) and 3 σ (dotted) cross sections for the ZA^0 signal required for an integrated luminosity (L) of (a) 30 fb^{-1} and (b) 300 fb^{-1} . We have applied the acceptance cuts as well as the tagging and mistagging efficiencies described in the text.

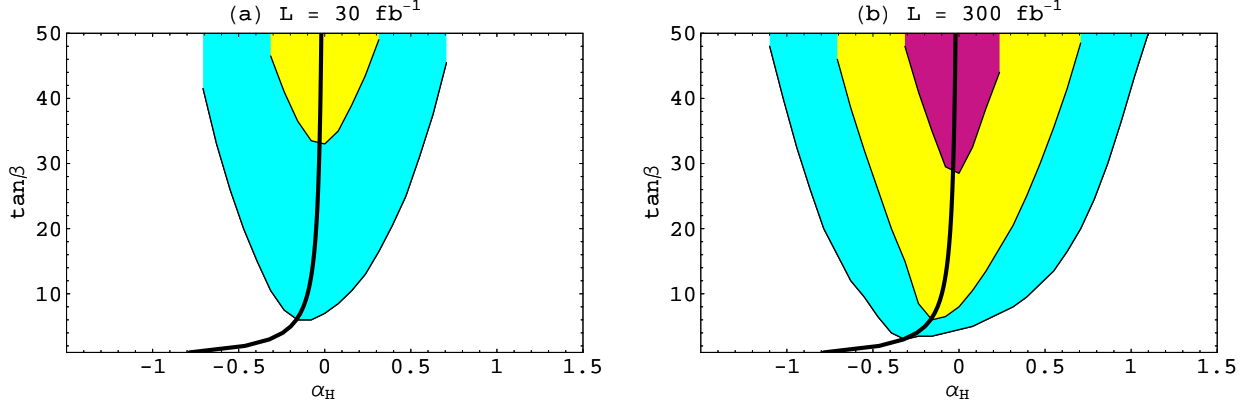


FIG. 5: The 5σ discovery contours at the LHC with an integrated luminosity (L) of (a) 30 fb^{-1} and (b) 300 fb^{-1} in the $(\alpha_H, \tan\beta)$ plane for $m_A = 150 \text{ GeV}$ (medium shading), $m_A = 250 \text{ GeV}$ (light shading), and 400 GeV (dark shading) in a two Higgs doublet model with $m_h = 120 \text{ GeV}$ and $m_H = m_A + 100 \text{ GeV}$. The discovery region is the part of the parameter space above the contours. In addition, we present the curve for the decoupling limit with $\beta - \alpha_H = \pi/2$. The Higgs signal includes contributions from $b\bar{b} \rightarrow ZA^0$ alone. We have applied the acceptance cuts as well as the tagging and mistagging efficiencies described in the text.